JMEPEG (2010) 19:873–879
DOI: 10.1007/s11665-009-9542-3

1059-9495/$19.00

Corrosion Mitigation of Copper in Acidic Chloride Pickling Solutions by 2-Amino-5-ethyl-1,3,4-thiadiazole

El-Sayed M. Sherif

(Submitted January 29, 2009; in revised form July 28, 2009)

Corrosion of copper in acidic chloride pickling solutions of 0.5 M HCl and its mitigation by 2-amino-5-ethyl-1,3,4-thiadiazole (AETDA) have been investigated using potentiodynamic polarization, chronoamperometry, electrochemical impedance spectroscopy (EIS), and weight-loss measurements. The study was also complemented by scanning electron microscopy (SEM), energy dispersive x-ray (EDX), and UV-Visible absorption spectroscopy investigations. The presence of AETDA and the increase of its concentration in the chloride solutions greatly decreased the corrosion rate and increased the surface and polarization resistances of copper as indicated by the electrochemical measurements. Weight-loss data also indicated that AETDA decreases the dissolution of copper coupons in the studied chloride solution. SEM/EDX investigations showed that AETDA molecules are strongly adsorbed onto copper surface. The UV-Visible absorption spectra confirmed that AETDA molecules suppress the corrosion of copper via their interactions with the copper surface via their adsorption then formation of AETDA-Cu complex.

Keywords 2-amino-5-ethyl-1,3,4-thiadiazole, copper corrosion, corrosion inhibitors, electrochemical and spectroscopic techniques, hydrochloric acid solutions

1. Introduction

Copper (Cu) has a wide range of applications due to its excellent thermal and electrical conductivities, mechanical workability, and good corrosion resistance. Copper has been commonly used in heat conductors, heat exchangers, as a material in heating and cooling systems, etc. (Ref 1-3). Both scale and corrosion products have negative effects on heat transfer and cause a decrease in the heating efficiency of the equipment, which requires periodic de-scaling and cleaning in hydrochloric acid (HCl) solution. It is well known that corrosion inhibitors effectively eliminate the undesirable destructive effects of the acid and prevent Cu dissolution. Consequently, the mechanisms of the anodic dissolution of Cu in HCl solutions and its inhibition have been investigated and different dissolution mechanisms have been proposed (Ref 4-18).

Owing to stricter environmental regulations, low inhibitor toxicity is an important requirement for the applied inhibitors. The latest trend in industry is to replace toxic inhibitors, such as triazoles, with nontoxic organic chemicals that can cause no harm to the environment. In closed systems, thiazole derivatives can act as an excellent replacement for the toxic triazoles (Ref 19). The inhibiting action of these organic compounds is usually attributed to their interactions with the Cu surface via their adsorption. Polar functional groups are regarded as the reaction center that stabilizes the adsorption process (Ref 14).

We have been studying corrosion and corrosion inhibition of Cu (Ref 2, 3, 5-7, 13-18) and aluminum (Ref 20, 21) as well as stainless steel alloys (Ref 22) in a variety of media. These studies have been carried out using different electrochemical, gravimetric, spectroscopic, and surface analyses investigations under different experimental conditions. This study reports the results obtained in studying the corrosion and corrosion inhibition of Cu in 0.5 M HCl solution by 2-amino-5-ethyl-1,3,4-thiadiazole (AETDA). This organic compound has shown high inhibition efficiency against Cu corrosion in sea water (Ref 18). AETDA is also expected to show powerful inhibition effectiveness versus the Cu corrosion in HCl because it is a heterocyclic compound containing a variety of donor atoms.

2. Experimental Details

AETDA (Sigma-Aldrich, 97%), HCl (Glassworld, 32%), and absolute ethanol (C_2H_5OH, Fisher, 99.9%) were used as received. An electrochemical cell with a three-electrode configuration was used; a Cu rod (Goodfellow, 99.999%, 5.0 mm in diameter), a platinum foil, and an Ag/AgCl electrode (in saturated KCl) were used as a working, counter, and reference electrodes, respectively. The Cu rods for electrochemical analysis were prepared by attaching an insulated Cu wire to one face of the sample using an aluminum conducting tape, and cold mounted in resin. The samples were then left to dry in air for 24 h at room temperature. To prevent the possibility of crevice corrosion during measurement, the interface between sample and resin was coated with Bostik Quickset, a polyacrylate resin. The Cu electrode was first polished successively with metallographic emery paper of

El-Sayed M. Sherif, Electrochemistry and Corrosion Laboratory, Department of Physical Chemistry, National Research Centre (NRC), Dokki, 12622 Cairo, Egypt and Center of Excellence for Research in Engineering Materials (CEREM), College of Engineering, King Saud University, P. O. Box 800, Riyadh 11421, Saudi Arabia. Contact e-mails: esherif@ksu.edu.sa and emsherif@gmail.com

increasing fineness of up to 600 grits, further with 5, 1, 0.5, and 0.3 μm alumina slurries (Fisher). The electrode was then washed with doubly distilled water, degreased with acetone, washed using doubly distilled water again, and finally dried with pure nitrogen.

Electrochemical experiments were performed by using an EG&G model 273A potentiostat-galvanostat. For potentiodynamic polarization experiments, the potential was scanned from −600 to 800 mV at a scan rate of 1 mV/s. Chronoamperometric experiments were carried out by stepping the potential at 200 mV for 120 min. A Philips model XL30SFEG scanning electron microscope (SEM) with an energy dispersive x-ray (EDX) analyzer attached was used for surface analysis of Cu in 0.5 M HCl containing 5.0×10^{-3} M AETDA for 120 min. For this purpose, the Cu sample was first removed from the inhibited chloride solution after performing a chronoamperometric experiment at 200 mV for 120 min, then rinsed in distilled water and finally dried with pure nitrogen. Impedance measurements were made using a Solatron SI 1255 HF frequency response analyzer along with the EG&G model 273A potentiostat-galvanostat. The instruments were controlled by the EG&G M398 software program between 100 kHz and 0.05 Hz with an ac wave of ±5 mV peak-to-peak overlaid on a dc bias potential, and the impedance data were obtained at a rate of 10 points per decade change in frequency. The impedance measurements were carried out at the open circuit potential after 60 min immersion of the Cu electrode in the test electrolyte.

The weight loss experiments were carried out using cylindrical Cu coupons (Goodfellow, 99.999%) having the dimensions, 5.10 cm diameter, 0.20 cm height, and exposed total area of 42.4 cm^2. The coupons were polished and dried as that in the case of Cu rods, then weighed, and suspended in 200 mL solution of 0.5 M HCl with and without the desired concentrations of AETDA. At the end of the run, the samples were rinsed with distilled water, dried, and weighed again. All weight-loss measurements were performed in triplicates and the maximum standard deviation in the observed weight loss was ±2%. The loss in weight (mg/dm^2), the corrosion rate (mg/dm^2/day, mdd), and the percentage of the inhibition efficiency over the exposure time were calculated as reported in our previous work (Ref 6, 7). UV-Visible absorption spectra were obtained on solutions before and after weight-loss experiments by using a SCINCO S-2000 UV-Visible spectrophotometer.

All solutions were prepared using doubly distilled water and ethanol (99:1, v/v), and all measurements were carried out at room temperature.

3. Results

3.1 Potentiodynamic Polarization Measurements

The potentiodynamic polarization curves of the Cu electrode in 0.5 M HCl solution without (a) and with 1.0×10^{-3} (b), 5.0×10^{-3} (c), and 1.0×10^{-2} M AETDA (d) are shown in Fig. 1. Anodic current of Cu in 0.5 M HCl in the absence of AETDA molecules (Fig. 1, curve a) displays three distinct regions: a Tafel region at lower over-potentials extending to the peak current density (j_{peak}), due to the dissolution of Cu into Cu^+; a region of decreasing currents until a minimum (j_{min}) is reached, due to formation of CuCl; and a region of sudden

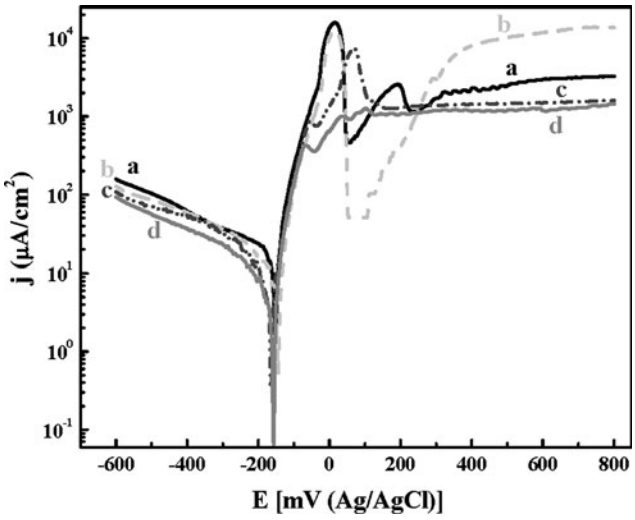

Fig. 1 Potentiodynamic polarization curves for the Cu electrode in 0.5 M HCl without (a) and with 1.0×10^{-3} (b), 5.0×10^{-3} (c), and 1.0×10^{-2} M AETDA (d)

increase in current density leading to a limiting value (j_{lim}), as a result of $CuCl_2^-$ formation (Ref 23).

In the presence of 1.0×10^{-3} M AETDA (Fig. 1, curve b), cathodic, corrosion (j_{Corr}), and anodic currents are noticed to decrease to the lower values as well as the values of corrosion potential (E_{Corr}) slightly shifted in the negative direction. This effect was noticeably increased with increasing the concentration of AETDA in the solution. The values of j_{peak}, j_{min}, cathodic (β_c) and anodic Tafel (β_a) slopes, j_{Corr}, E_{Corr}, polarization resistance (R_p), corrosion rate (k_{Corr}), degree of surface coverage (θ), and the inhibition efficiency (IE%) obtained from Fig. 1 are listed in Table 1. The values of j_{Corr}, E_{Corr}, R_p, K_{Corr}, IE%, and θ were obtained according to the previous studies (Ref 24-27). It is obvious from Table 1 that the values of j_{Corr}, j_{peak}, j_{min}, and k_{Corr} decrease and E_{Corr} slightly shifts in the negative direction, while β_c, β_a, R_p, θ, and IE% increase in the presence of AETDA molecules. It is also seen from Table 1 that IE% of AETDA increases from ~44% at 1×10^{-3} to ~67% at 1×10^{-2} M.

3.2 Chronoamperometric Measurements and SEM/EDX Investigations

The variation of current values of Cu electrode with time at 200 mV versus Ag/AgCl in 0.5 M HCl in absence (a) and presence of 1.0×10^{-3} (b), 5.0×10^{-3} (c), and 1.0×10^{-2} M AETDA (d) are shown in Fig. 2. It can be seen from Fig. 2 that the highest current values for Cu obtained in the acid solution in the absence of AETDA agrees with the potentiodynamic polarization behavior (Fig. 1, curve a) at the same potential value. At the early stages of the run, the current decreased rapidly from about 32 to ~4 mA/cm^2 after which the current started to increase again accompanied by some little fluctuations, especially after the first 60 min of the run.

Addition of 1.0×10^{-3} M AETDA to the chloride solution (Fig. 2, curve b) greatly lowered the absolute currents at the whole time of the experiment. Further decreases were also measured when the concentration of AETDA was increased from 1.0×10^{-3} up to 1.0×10^{-2} M. The SEM micrograph

Table 1 Parameters obtained from potentiodynamic polarization curves shown in Fig. 1 for Cu electrode in 0.5 M HCl solutions in the absence and presence of 1.0×10^{-3}, 5.0×10^{-3}, and 1.0×10^{-2} M AETDA

Parameter solution	β_c, mV/dec	E_{Corr}, mV	β_a, mV/dec	j_{Corr}, μA/cm^2	j_{peak}, μA/cm^2	j_{min}, μA/cm^2	R_p, kΩ cm^2	K_{Corr}, mpy	θ	IE%
0.50 M HCl	130	−153	35	18	16,500	470	0.67	8.25	...	...
1.0×10^{-3} M AETDA added	160	−156	39	10.5	12,500	50	1.30	4.81	0.45	44.6
5.0×10^{-3} M AETDA added	190	−162	47	7.8	880	750	2.21	3.58	0.57	56.7
1.0×10^{-2} M AETDA added	212	−165	56	5.9	420	370	3.26	2.70	0.67	67.2

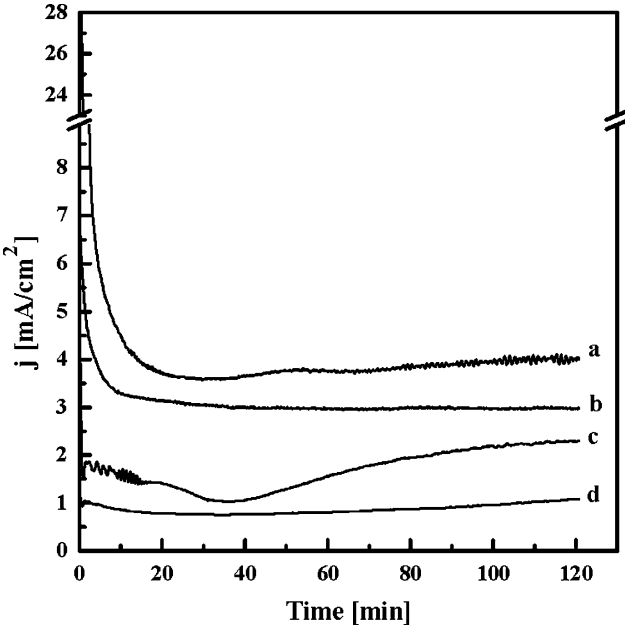

Fig. 2 Potentiostatic current-time curves for Cu electrode at 200 mV in 0.5 M HCl in the absence (a) and presence of 1.0×10^{-3} (b), 5.0×10^{-3} (c), and 1.0×10^{-2} M AETDA (d)

obtained for the Cu surface after stepping the potential to 200 mV in 0.5 M HCl containing 5.0×10^{-3} M AETDA for 120 min is shown in Fig. 3(a) in which there are two areas: (I) and (II). The EDX profile analysis corresponding to area (I) of Fig. 3(a) is shown in Fig. 3(b), where the atomic percentage of the detected elements represent 23.62% C, 10.30% N, 2.4% S, 40.14% Cu, and 21.36% Cl. This indicates that the AETDA molecules at this area are adsorbed partially on the Cu surface as the percents of Cu and Cl still high. An expanded version of the area (II) in Fig. 3(a) is shown in Fig. 4(a), which depicts that the whole Cu surface at this area is covered up with the AETDA molecules. This was also confirmed by the EDX profile analysis that was taken for the area shown in the Fig. 4(a) and presented in Fig. 4(b). The atomic percent of the elements in this area recorded 48.41% C, 21.19% N, and 7.01% S, while the percent for Cl and Cu was only 6.99 and 15.28%.

3.3 Electrochemical Impedance Spectroscopy (EIS) Measurements

To determine the impedance characteristics at the Cu/electrolyte interface under various experimental conditions, EIS measurements were carried out. The Nyquist impedance plots obtained for the Cu electrode at open-circuit potential after 60 min immersion in solution of 0.5 M HCl without (1) and

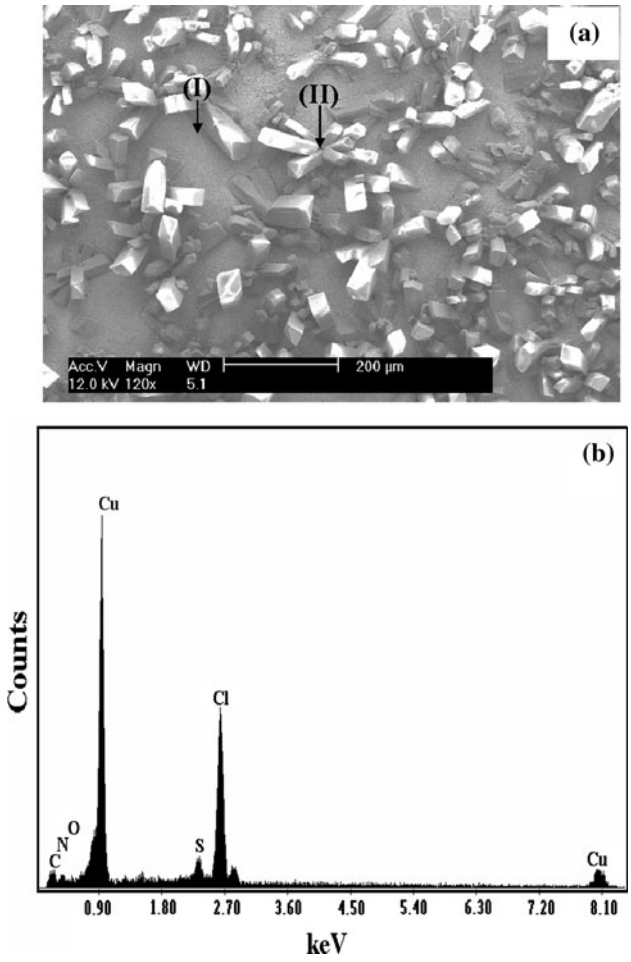

Fig. 3 (a) SEM image of the Cu surface obtained after stepping the potential to 200 mV in 0.5 M HCl containing 5.0×10^{-3} M AETDA for 120 min and (b) the corresponding EDX profile analysis of the area (I) shown in the image

with 1.0×10^{-3} (2), 5.0×10^{-3} (3), and 1.0×10^{-2} M AETDA (4) are shown in Fig. 5(a). Symbols represent the measured data and solid lines represent the best fit using the equivalent circuit shown in Fig. 5(b). Figure 5(c) shows the total polarization resistance ($R_{p1} + R_{p2}$) plotted as a function of the inhibitor concentration. The parameters obtained by fitting the equivalent circuit shown in Fig. 5(b) are listed in Table 2, where R_S represents the solution resistance, R_{p1} is the polarization resistance, Q is the constant phase elements (CPEs), W is the Warburg impedance, C_{dl} is the double layer capacitance, and R_{p2} is another polarization resistance. It can be seen from Fig. 5(a) and Table 2 that the increase in AETDA

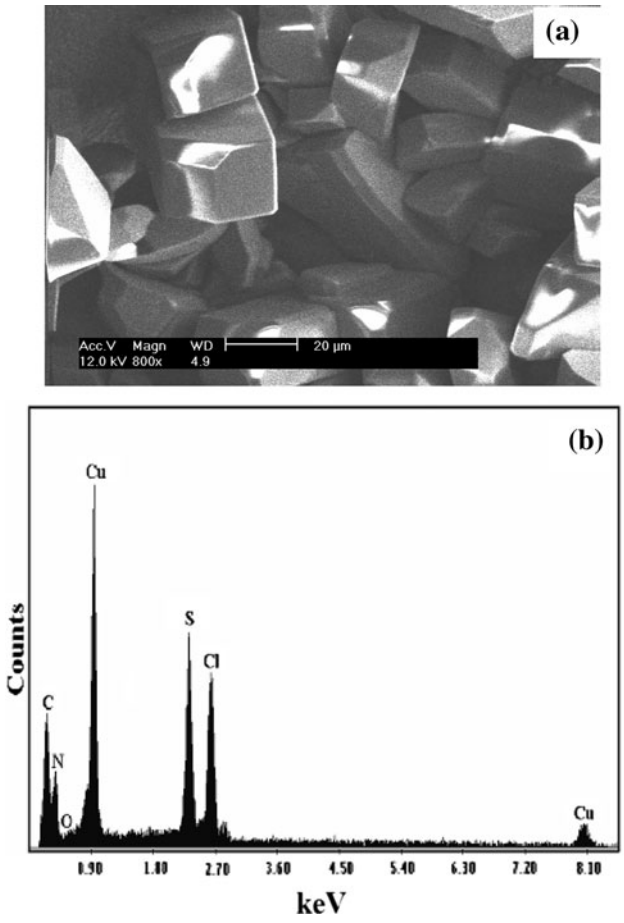

Fig. 4 (a) An expanded version of the SEM area (II) that is shown in Fig. 3(a) and (b) the corresponding EDX profile analysis of the area shown in the image

concentrations raises the solution resistance, R_S, and the polarization resistances, R_{p1} and R_{p2}. The CPEs (Q) are almost like Warburg impedance when their n values are close to 0.5 and are like double layer capacitors with some pores when n values reaches 1.0; the CPEs decrease upon addition of AETDA and upon the increase in its concentration. It has been reported (Ref 28) that the semicircles at high frequencies are generally associated with the relaxation of electrical double layer capacitors, and the diameters of the high-frequency capacitive loops can be considered as the charge transfer resistance. The inhibition efficiency (IE%) of AETDA for the Cu electrode can be calculated from the charge transfer resistance as follows:

$$\mathrm{IE}\% = \left[\frac{R_{p1} - R^{o}_{p1}}{R_{p1}}\right] \times 100 \qquad \text{(Eq 1)}$$

where R_{p1} and R^{o}_{p1} are the charge transfer resistances in 0.5 M HCl with and without AETDA, respectively. The values of this calculated IE% are listed in Table 2 from which it is also seen that the value of IE% increases as the concentration of AETDA increases in the solution. This agrees with the IE% values obtained by potentiodynamic polarization (Table 1) and current-time. The presence of the Warburg (W) impedance indicates that the mass transport is limited by the surface adsorbed layer on the Cu surface. The presence of double layer capacitance (C_{dl}) and the decrease of its value

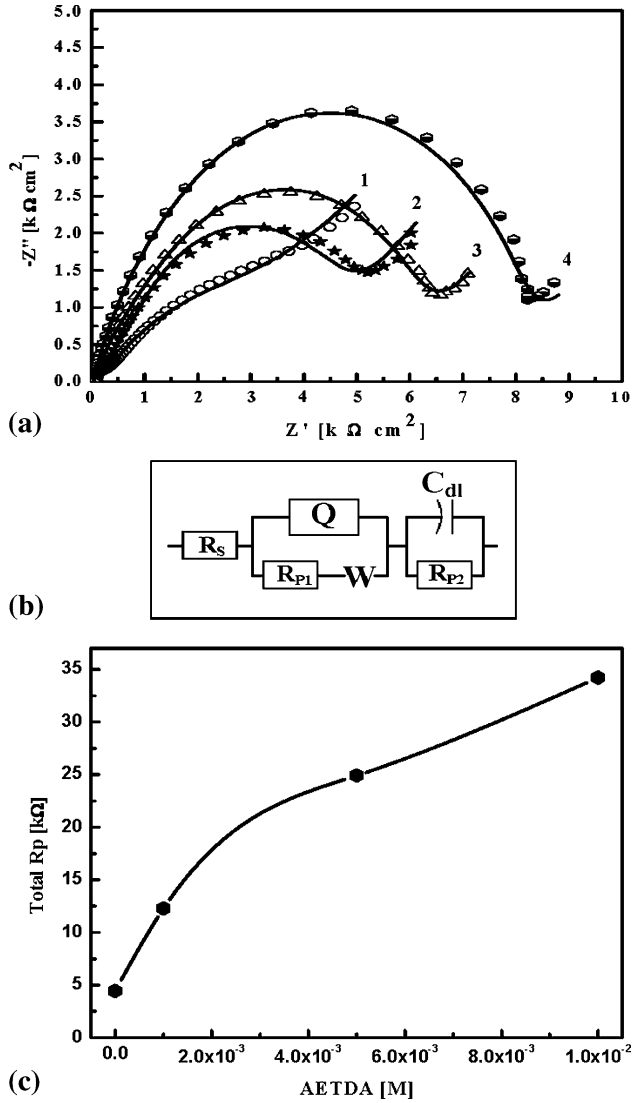

Fig. 5 (a) Nyquist plots for the Cu electrode after 60 min immersion in 0.5 M HCl in the absence (1) and presence of 1.0×10^{-3} (2), 5.0×10^{-3} (3), and 1.0×10^{-2} M AETDA (4); (b) the equivalent circuit used to fit the experimental data presented in Fig. 5(a); and (c) polarization resistances plotted as a function of the AETDA concentration

with the increase of AETDA concentrations, which is expected to cover-up the charged surfaces reducing the capacitive effects and suggest also that the electron transfer reaction corresponding to the second semicircle takes place through the surface layer, which limits mass transport or acts just like another resistor.

3.4 Weight-Loss Measurements

The weight losses versus time for the Cu coupons in 200 mL of 0.5 M HCl in absence (1) and presence of 1.0×10^{-3} (2), 5.0×10^{-3} (3), and 1.0×10^{-2} M AETDA (4) are shown in Fig. 6(a). Figure 6(a, curve 1) shows that the weight loss of Cu recorded ~0.75 mg/dm^2 after 2 h and increased linearly to record ~3.5 mg/dm^2 in 12 h. Addition of 1.0×10^{-3} M AETDA (Fig. 6a, curve 2) lowered the weight loss to a significant extent even after 12 h in comparison to that obtained in the case of HCl alone. Increasing the concentration

Table 2 EIS parameters obtained by fitting the Nyquist plots shown in Fig. 5(a) with the equivalent circuit shown in Fig. 5(b) for Cu electrode in 0.5 M HCl solutions in the absence and presence of AETDA

		Q						
Parameter solution	R_s, Ω	Y_Q, μF/cm^2	*n*	R_{p1}, kΩ	*W*, Ω/s$^{1/2}$	C_{dl}, μF/cm^2	R_{p2}, kΩ	IE%
0.50 M HCl	31.5	0.96	0.57	4.28	5.29E−5	96.8	0.165	···
1.0×10^{-3} M AETDA added	33.58	0.427	0.65	11.11	6.1E−5	0.35	3.18	61.5
5.0×10^{-3} M AETDA added	41.4	0.326	0.70	21.05	9.78E−5	0.25	3.86	79.7
1.0×10^{-2} M AETDA added	43.42	0.306	0.77	28.14	13.3E−5	0.15	6.10	84.8

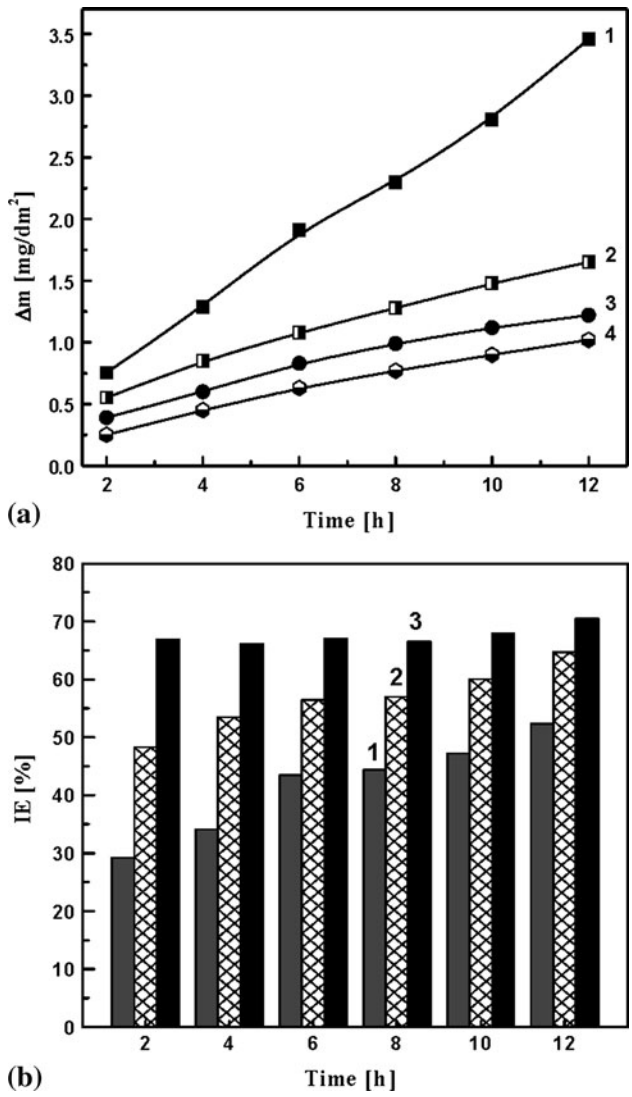

Fig. 6 Variation of (a) the weight loss with time for Cu coupons in 0.5 M HCl in the absence (1), presence of 1.0×10^{-3} (2), 5.0×10^{-3} (3), and 1.0×10^{-2} M AETDA (4) and (b) the inhibition efficiency (IE%) with time for Cu coupons in 0.5 M HCl containing 1.0×10^{-3} (1), 5.0×10^{-3} (2), and 1.0×10^{-2} M AETDA (3)

of AETDA to 5.0×10^{-3} M, curve 3, represented further decrease in the weight loss, while the minimum weight loss was obtained when the concentration was increased to 1.0×10^{-2} M, curve 4. Perhaps, the adsorption of AETDA molecules onto the Cu surface limits the dissolution of Cu.

This was also indicated by plotting the variation of the inhibition efficiency (IE%) that was calculated from the loss in weight of the Cu specimens by AETDA with time as shown in Fig. 6(a). The values of IE% were calculated according to the following equation (Ref 13-15),

$$\text{IE\%} = \frac{K_{\text{Corr}}^{\text{un}} - K_{\text{Corr}}^{\text{in}}}{K_{\text{Corr}}^{\text{un}}} \times 100 \qquad \text{(Eq 2)}$$

The inhibition efficiency of 1.0×10^{-3} M AETDA recorded about 52% after 12 h, increased to about 65% at 5.0×10^{-3} and 71% when the concentration was increased to 1.0×10^{-2} M. This emphasizes the fact that the presence of AETDA precludes the dissolution of Cu and this effect increases upon increasing the AETDA concentration.

3.5 UV-Visible Absorption Spectra

Figure 7 represents the UV-Visible absorption spectra of the solutions containing: (a) 0.5 M HCl; and (b) 0.5 M HCl + 5.0×10^{-3} M AETDA before Cu immersion (1) and after 12 h immersion (2), respectively. These experiments were carried out to confirm the possibility of the formation of AETDA-Cu(1) complex in the test electrolyte. The chloride solution (Fig. 7a) before Cu immersion (curve 1) shows only one weak band at 233 nm, while after 12 h immersion of Cu (curve 2), several absorption bands across the spectrum particularly at about 204, 211, 216, and 256 nm appear. On the other hand, the absorption spectrum of the solution containing 5.0×10^{-3} M AETDA shown in Fig. 7(b) before the Cu immersion (curve 1) shows a sharp band at 203 nm and another one at 248 nm. These bands shifted to 208 and 243 nm, respectively, after 12 h of Cu immersion (curve 2). This is because the amine groups of AETDA are strongly held up in the formation of a complex with Cu^+. It has been reported that Cu forms such complex with 2-amino-thiazole (Ref 29) as well as many other azole derivatives (Ref 4, 15, 30, 31).

4. Discussion

It is well known that the anodic reaction of Cu, when the concentration of HCl < 1 M, is the dissolution of Cu through oxidation of Cu(0) to Cu^+ then Cu^+ to Cu^{2+} (Ref 32). According to Braun and Nobe (Ref 9), Cu^+ reacts with chloride ion from the solution as follows:

$$Cu^+ + Cl^- = CuCl \qquad \text{(Eq 3)}$$

This CuCl does not produce enough protection to the Cu surface and transforms to the soluble cuprous chloride complex, $CuCl_2^-$ (Ref 8),

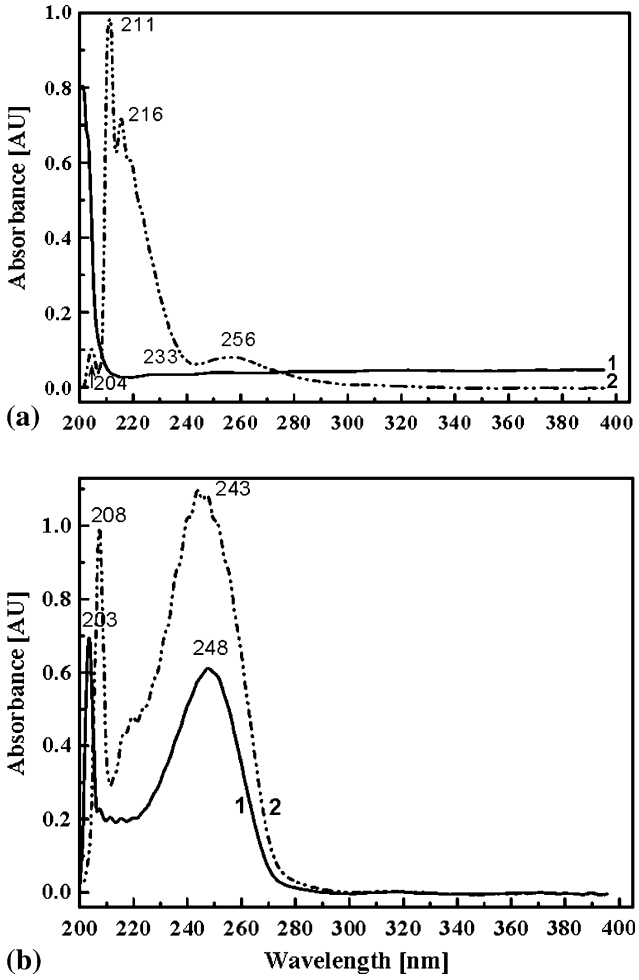

Fig. 7 UV-Visible absorption spectra of the solutions containing: (a) 0.5 M HCl before Cu immersion (1) and after 12 h immersion (2); and (b) 0.5 M HCl + 5.0×10^{-3} M AETDA before Cu immersion (1) and after 12 h immersion (2). The spectra were taken after the original solution was diluted by a factor of 1:5

$$CuCl + Cl^- = CuCl_2^- \quad \text{(Eq 4)}$$

If $CuCl_2^-$ is adsorbed on the surface, its dissolution into the bulk solution or its further oxidation to cupric ions (Ref 8, 9) will occur according to Eq. 5 and/or Eq. 6,

$$CuCl_2^-(\text{surface}) = CuCl_2^-(\text{solution}) \quad \text{(Eq 5)}$$

$$CuCl_2^-(\text{surface}) = Cu^{2+} + 2Cl^- + e^- \quad \text{(Eq 6)}$$

The overall corrosion reaction of Cu in acidic chloride solution in the absence of an inhibitor at this condition can be represented as follows (Ref 4):

$$2Cu + 4HCl + O_2 = 2Cu^{2+} + 4Cl^- + 2H_2O \quad \text{(Eq 7)}$$

The decrease of J_{Corr}, J_{peak}, J_{min}, and k_{Corr} and the increase of R_p, θ, and IE% values in the presence of AETDA (Fig. 1) are mainly due to the decrease of the Cu electrodissolution. The negative shift in the E_{Corr} with the increase in the AETDA concentration is clearly shown by the increase in the β_c values, as a result of the ability of the adsorbed AETDA layer to inhibit the cathodic reaction. Furthermore, the increase of both β_c and β_a values relates to the decrease in both the cathodic and anodic currents. The electrodissolution of Cu in the presence of AETDA could take place as reported for other inhibitors, electro-oxidize primarily to Cu^+ and is able to form a slightly soluble $Cu^+(AETDA)^-$ complex as the main electrodeposition products in the presence of a clean surface, i.e., in the case of Cu/Cu_2O system (Ref 33).

$$Cu^+ = Cu^{2+} + e^- \quad (\text{slow reaction}) \quad \text{(Eq 8)}$$

The reaction of the inhibitor molecules and the Cu surface can be then explained as follows:

$$CuCl_2^- + AETDA + e^- = Cu^+(AETDA)^- + 2Cl^- \quad \text{(Eq 9)}$$

This was also demonstrated by SEM and EDX investigations shown in Fig. 3 and 4. Although a few of Cl^- is still present in the structure of the inhibition film, the AETDA molecules adsorbed strongly on the Cu forming a $Cu^+(AETDA)^-$ complex, preventing Cu surface from being corroded easily. This also explains the decrease of current values shown in Fig. 2, as the concentration of AETDA increases in the solution. It is interesting to note also that the total polarization resistance obtained from EIS is greatly increased by the inhibitor concentration as shown in Fig. 5c, which gives indication that the inhibitor forms a layer, which grows upon increasing the AETDA concentration and behaves as a resistor for the electron transfer. That is, the layer becomes thicker in direct proportion to the concentration of AETDA, to which the corrosion rate is inversely proportional. Also, the increased values of R_S proved that the solution resistance increases with increasing AETDA content in the solution. Moreover, the positive identification of the complex in the solution by UV-Visible absorption spectra (Fig. 7b) confirms that AETDA plays an important role in protecting the Cu surface against the aggressiveness of the acid solution. All these results indicate that AETDA is a good corrosion inhibitor for Cu in HCl solution and its ability increases with its concentration.

5. Conclusions

The corrosion of Cu in 0.5 M HCl solution and its inhibition by AETDA using electrochemical, gravimetric, and spectroscopic measurements has been carried out. Polarization and EIS measurements indicated that the presence of AETDA and the increase of its concentration decrease, to a great extent, the cathodic, corrosion, and anodic currents and corrosion rates of Cu as well as increase surface and polarization resistances. Current-time and SEM/EDX investigations revealed that AETDA inhibits Cu surface even at high potential values (200 mV) due to the adsorption of AETDA onto the surface. The maximum inhibition efficiency obtained by weight loss after 12 h of Cu immersion at 1.0×10^{-3} M AETDA is about 52% and increased to ~65% at 5.0×10^{-3} M and 71% at 1.0×10^{-2} M. UV-Visible absorption spectroscopy identified the presence of AETDA-Cu complex in the chloride solution containing AETDA.

References

1. L. Núńez, E. Reguera, F. Corvo, E. Gonzalez, and C. Vazquez, Corrosion of Copper in Seawater and Its Aerosols in a Tropical Island, *Corros. Sci.*, 2005, **47**, p 461
2. A. El Warraky, H.A. El Shayeb, and E.M. Sherif, Pitting Corrosion of Copper in Chloride Solutions, *Anti-Corros. Methods Mater.*, 2004, **51**, p 52
3. E.M. Sherif, R.M. Erasmus, and J.D. Comins, Corrosion of Copper in Aerated Synthetic Sea Water Solutions and Its Inhibition by 3-Amino-1, 2, 4-triazole, *J. Colloid Interface Sci.*, 2007, **309**, p 470
4. D.-Q. Zhang, L.-X. Gao, and G.-D. Zhou, Inhibition of Copper Corrosion by Bis-(1-benzotriazolymethylene)-(2,5-thiadiazoly)-disulfide in Chloride Media, *J. Appl. Surf. Sci.*, 2004, **225**, p 287
5. E.M. Sherif, R.M. Erasmus, and J.D. Comins, Corrosion of Copper in Aerated Acidic Pickling Solutions and Its Inhibition by 3-Amino-1, 2, 4-triazole-5-thiol, *J. Colloid Interface Sci.*, 2007, **306**, p 96
6. E.M. Sherif and S.-M. Park, Inhibition of Copper Corrosion in Acidic Pickling Solutions by N-phenyl-1, 4-phenylenediamine, *J. Electrochem. Acta*, 2006, **51**, p 4665
7. E.M. Sherif and S.-M. Park, Effects of 2-Amino-5-ethylthio-1, 3, 4-thiadiazole on Copper Corrosion as a Corrosion Inhibitor in Aerated Acidic Pickling Solutions, *J. Electrochem. Acta*, 2006, **51**, p 6556
8. F.K. Crundwell, The Anodic Dissolution of Copper in Hydrochloric Acid Solutions, *J. Electrochim. Acta*, 1992, **37**, p 2707
9. M. Braun and K. Nobe, Electrodissolution Kinetics of Copper in Acidic Chloride Solutions, *J. Electrochem. Soc.*, 1979, **126**, p 1666
10. E.M. Sherif, R.M. Erasmus, and J.D. Comins, Inhibition of Copper Corrosion in Acidic Chloride Pickling Solutions by 5-(3-Aminophenyl)-tetrazole as a Corrosion Inhibitor, *Corros. Sci.*, 2008, **50**, p 3439
11. H.P. Lee and K. Nobe, Kinetics and Mechanisms of Cu Electrodissolution in Chloride Media, *J. Electrochem. Soc.*, 1986, **133**, p 2035
12. H.P. Lee, K. Nobe, and A.J. Pearlstein, Film Formation and Current Oscillations in the Electrodissolution of Cu in Acidic Chloride Media, *J. Electrochem. Soc.*, 1985, **132**, p 1031
13. E.M. Sherif and S.-M. Park, Inhibition of Copper Corrosion in 3.0% NaCl Solution by N-phenyl-1, 4-phenylenediamine, *J. Electrochem. Soc.*, 2005, **152**, p B428
14. E.M. Sherif, Effects of 2-Amino-5-(ethylthio)-1,3,4-thiadiazole on Copper Corrosion as a Corrosion Inhibitor in 3% NaCl Solutions, *J. Appl. Surf. Sci.*, 2006, **252**, p 8615
15. E.M. Sherif and S.-M. Park, 2-Amino-5-ethyl-1, 3, 4-thiadiazole as a Corrosion Inhibitor for Copper in 3.0% NaCl Solutions, *Corros. Sci.*, 2006, **48**, p 4065
16. E.M. Sherif, A.M. El Shamy, M.M. Ramla, and A.O.H. El Nazhawy, 5-(Phenyl)-4H-1,2,4-triazole-3-thiol as a Corrosion Inhibitor for Copper in 3.5% NaCl Solutions, *Mater. Chem. Phys.*, 2007, **102**, p 231
17. E.M. Sherif, R.M. Erasmus, and J.D. Comins, Inhibition of Corrosion Processes on Copper in Aerated Sodium Chloride Solutions by 5-(3-Aminophenyl)-tetrazole, *Appl. Electrochem.*, 2009, **39**, p 83
18. E.M. Sherif, R.M. Erasmus, and J.D. Comins, Effects of 3-Amino-1, 2, 4-triazole on the Inhibition of Copper Corrosion in Acidic Chloride Solutions, *J. Colloid Interface Sci.*, 2007, **311**, p 144
19. Gy. Vastag, E. Szöcs, A. Shaban, and E. Kálmán, New Inhibitors for Copper Corrosion, *Pure Appl. Chem.*, 2001, **73**, p 1861
20. E.M. Sherif and S.-M. Park, Effects of 1,5-Naphthalenediol on Aluminum Corrosion as a Corrosion Inhibitor in 0.50 M NaCl, *J. Electrochem. Soc.*, 2005, **152**, p B205
21. E.M. Sherif and S.-M. Park, Effects of 1,4-Naphthoquinone on Aluminum Corrosion in 0.50 M Sodium Chloride Solutions, *Electrochim. Acta*, 2006, **51**, p 1313
22. J.H. Potgieter, P.A. Olubambi, L. Cornish, C.N. Machio, and E.M. Sherif, Influence of Nickel Additions on the Corrosion Behaviour of Low Nitrogen 22% Cr Series Duplex Stainless Steels, *Corros. Sci.*, 2008, **50**, p 2572
23. L. Bacarella and J.C. Griess, Anodic Dissolution of Cu in Flowing NaCl Solutions Between 25 and 175°C, *J. Electrochem. Soc.*, 1973, **120**, p 459
24. P.R. Roberge, *Handbook of Corrosion Engineering*, McGraw-Hill, New York, 2000
25. J.R. Scully, Polarization Resistance Method for Determination of Instantaneous Corrosion Rates, *Corrosion*, 2000, **56**, p 199
26. M. Metikoš-Huković, R. Babić, and Z. Grubać, Corrosion Protection of Aluminium in Acidic Chloride Solutions with Nontoxic Inhibitors, *J. Appl. Electrochem.*, 1998, **28**, p 433
27. C.W. Yan, H.C. Lin, and C.N. Cao, Investigation of Inhibition of 2-Mercaptobenzoxazole for Copper Corrosion, *Electrochim. Acta*, 2000, **45**, p 2815
28. H.Y. Ma, S. Chen, L. Niu, S. Zhao, S. Li, and D. Li, Inhibition of Copper Corrosion by Several Schiff Bases in Aerated Halide Solutions, *J. Appl. Electrochem.*, 2002, **32**, p 65
29. F.H. AL-Hajjar and F.M. AL-Kharafi, 2-Amino-thiazole and 2-Amino-4,6-dimethylpyrimidine as Corrosion Inhibitors for Copper, *Corros. Sci.*, 1988, **28**, p 163
30. E. Geler and D.S. Azambuja, Corrosion Inhibition of Copper in Chloride Solutions by Pyrazole, *Corros. Sci.*, 2000, **42**, p 631
31. V. Lakshminarayanan, R. Kannan, and S.R. Rajagopalan, Cyclic Voltammetric Behavior of Certain Copper-Azole Systems Using Carbon Paste Electrodes, *J. Electroanal. Chem.*, 1994, **364**, p 79
32. G. Moretti and F. Guidi, Tryptophan as Copper Corrosion Inhibitor in 0.5 M Aerated Sulfuric Acid, *Corros. Sci.*, 2002, **44**, p 1995
33. G. Trabanelli, Inhibitors—An Old Remedy for a New Challenge, *Corrosion*, 1991, **47**, p 410